

The Concept of Photozymes: Short Peptides with Photoredox Catalytic Activity for Nucleophilic Additions to α -Phenyl Styrenes

Daniel Sack^[a] and Hans-Achim Wagenknecht^{*[a]}*In memory of Klaus Hafner*

Conventional photoredox catalytic additions of alcohols to olefins require additives, like thiophenol, to promote back electron transfer. The concept of “photozymes” assumes that forward and backward electron transfer steps in a photoredox catalytic cycle are controllable by substrate binding to photocatalytically active peptides. Accordingly, we synthesized a short tripeptide modified with 1,7-dicyano-perylene-3,4:9,10-tetracarboxylic acid bisimide as photoredox catalyst. This peptide undergoes an unconventional photoredox catalytic cycle with

the radical anion and dianion of the perylene bisimide-peptide as intermediates. The photoredox catalytic reactions with α -phenyl styrenes as substrates require remarkably low catalyst loadings (0.5 mol%) and give the methoxylation products in high yields. The concept of “photozymes” for photoredox catalysis has significant potential for other photocatalytic reactions, in particular with respect to enantioselective photocatalysis.

Introduction

Peptides, especially those with only less than ten amino acids, are an established type of catalysts for important classes of organic reactions, including oxidations, reductions, group transfers, like acylations, additions and C–C-bond formation, in particular aldol reactions.^[1] In many cases, asymmetric transformations were realized and short peptides are considered more as organocatalysts than as small enzymes. In comparison with enzymes, the catalytic potential of small peptides is astonishing regarding their rather simple structure. The main advantages of short peptides are the good accessibility by synthesis and their good solubility in both organic and aqueous solutions. Short peptides were only rarely used for photochemical transformations and as photoredox catalysts. The very few examples include peptides as models for DNA photolyase activity to cleave cyclobutane pyrimidine dimers^[2] and our pyrene-modified peptides as photoredox catalysts and the first “photozymes”.^[3] This is surprising, since photocatalysis with peptides offers new possibilities to use UV or visible light as “green” and cheap energy source to overcome activation

barriers of reactions by alternative pathways that are not accessible by the conventional thermal approach.^[4]

In general, photoredox catalysis has become a powerful method in modern synthetic organic chemistry. Furthermore, photoredox catalysis complements the available synthetic methods by so far unknown transformations and thereby overcomes limits of current synthetic methods.^[5] Transition metal complexes mainly with ruthenium are the mainly applied photoredox catalyst due to their photophysical properties and their (photo)chemical robustness.^[6] In order to enhance the sustainability by combining light from energy-saving LEDs and non-metallated photoredox catalysts, organic dyes are important alternatives, for instance, eosin y,^[7] flavins,^[8] rhodamine 6G,^[9] mesityl^[10] and aminoacridinium,^[11] naphthochromenones,^[12] perylene bisimides (PBIs)^[13] and dicyanobenzenes.^[14] However, there is not *one* single organic photoredox catalyst applicable for a variety of different types of organic reactions.^[15] Instead, each organic photoredox catalyst has its own reactivity profile and substrate scope. For nucleophilic additions of alcohols to alkenes, we established 1-(*N,N*-dimethylamino)pyrene,^[16] *N*-phenylphenothiazines^[17] and 1,7-dicyano-perylene-3,4:9,10-tetracarboxylic acid bisimides^[16] as organic photoredox catalysts to convert aromatic alkenes to products with Markovnikov- and anti-Markovnikov orientation, respectively. Most of these photocatalytic alcohol additions require additives, in particular thiophenol for products with anti-Markovnikov orientation, to promote back electron transfer from the radical intermediate (after alcohol addition) to the photocatalyst that closes the photoredox catalytic cycle and improves the product yields.^[16,18] An additive and H-atom donor is also crucial for the anti-Markovnikov hydrofunctionalizations of alkenes with mesityl acridinium as photoredox catalysts.^[10] In principle, an H atom transfer consists of a proton and an electron transfer in one step. However, thiophenol is a

[a] D. Sack, Prof. Dr. H.-A. Wagenknecht
Institute of Organic Chemistry
Karlsruhe Institute of Technology (KIT)
Fritz-Haber-Weg 16, 76131 Karlsruhe, Germany
E-mail: Wagenknecht@kit.edu
www.ioc.kit.edu/wagenknecht/

Supporting information for this article is available on the WWW under <https://doi.org/10.1002/ejoc.202101068>

Part of the “Special Collection in Memory of Klaus Hafner”.

© 2021 The Authors. European Journal of Organic Chemistry published by Wiley-VCH GmbH. This is an open access article under the terms of the Creative Commons Attribution License, which permits use, distribution and reproduction in any medium, provided the original work is properly cited.

nucleophile itself and may compete with the alcohols as desired nucleophile in side reactions. In principle, forward and backward electron transfer might be also controllable by substrate binding to photocatalytically active peptides. We call these peptides “photozymes” and established this new concept by short proline-rich peptides modified with 1-(*N,N*-dimethylamino)pyrene as photoredox active chromophore, such as **P0**, that catalyze nucleophilic additions of alcohols to α -phenyl styrenes to products with Markovnikov orientation (Figure 1). Herein, we extend the concept of “photozymes” to the nucleophilic addition of methanol to α -phenyl styrenes into products with anti-Markovnikov orientation. We present the short peptide **P1** modified with 1,7-dicyano-perylene-3,4:9,10-tetracarboxylic acid bisimide as photoredox catalyst. We provide important mechanistic insights how this “photozyme” work efficiently without thiophenol as additive reagent.

Results and Discussion

For the oxidative mode of photocatalytic alcohol addition to alkenes into anti-Markovnikov-oriented products, 1,7-dicyano-perylene-3,4:9,10-tetracarboxylic acid bisimide is an excellent photocatalysts and even better than mesitylacridinium.^[16] The two cyano groups of the perylene bisimide **1** are crucial for the desired photoredox catalytic activity. The 2,6-diisopropylphenyl substituents at the imide nitrogens prevent aggregation and thus enhance the solubility of this photoredox catalyst. They are typically introduced as final step of the chromophore synthesis

by Pd-catalyzed coupling with Zn(CN)₂. However, such Pd catalysis would interfere with the propargyl group that is needed at one of the perylene bisimide nitrogens for peptide conjugation by the copper(I)-catalyzed cycloaddition. We failed to introduce the cyano groups into dibrominated perylene anhydride precursors prior to the imide functionalizations with the propargyl amine. Hence, we decided to use the dibrominated perylene bisimide precursors **5** for conjugation. The building block **5** was synthesized in a stepwise procedure because the one-pot reaction failed in this case due to the different reactivity of the two different amines^[19] One of the anhydride groups of **3** was opened to the monopotassium salt, the imide group with propargylamine was introduced at the remaining anhydride and the dicarboxylic acid was closed again to the anhydride with hydrochloric acid to give the intermediate compound in 90% raw yield. The second amine was subsequently introduced in propionic acid under reflux in 20% yield. To obtain the photocatalytically active compounds, **7** was coupled by copper(I)-catalyzed cycloaddition to β -azido-L-alanine to **8** in 87% yield and further modified with the two cyano groups to the PBI-amino acid **9** in 92% yield. **5** was also conjugated to the presynthesized peptide **P2** in 90% yield and finally peptide **P3** was modified with the two cyanide groups in 56% yield to the final peptide **P1**. Both target compounds, **9** and **P1**, were purified by flash column chromatography and fully characterized by NMR spectroscopy and HR mass spectrometry (see Supporting Information). **P1** has the PBI-modified alanine at the C-terminus and L-arginine (Arg) at the N-terminus (Figure 2). According to our previous studies, this sequence together with a proline-type turn improves photoredox catalysis, but a longer proline chain is not required.^[3a] The Tos and Boc groups at the N-terminal arginine and the methyl esters at the C-terminal CN-PBI-modified alanine remained on the peptides to improve their solubility in MeCN as preferred solvent for photoredox catalysis.

PBI **1** served as reference chromophore for the optical and electrochemical characterization of peptide **P1**. It was synthesized according to literature.^[20] The UV/Vis absorption of all three compounds **1**, **9** and **P1** in MeCN show the PBI-typical maxima at 488 nm and 524 nm that fits perfectly to the green light-emitting diode (525 nm) as light source for photocatalysis (Figure 3). The extinction of **1** and **P1** is nearly identical; only the extinction of **9** is slightly diminished, probably as a result of some aggregation due to the missing 2,6-diisopropylphenyl substituent at one of the imide nitrogens. The aggregation is indicated by the small extinction increase at the peak borders between 400 and 450 nm and between 550 nm and 600 nm. The emission shows expectedly mirror-shape spectra with maxima at 545 nm (for **9** and **P1**) and 537 nm (for **1**). The emission intensity of **1** is significantly reduced in comparison to the emission intensities of **9** and **P1**. This could be due to a fluorescence quenching effect by the aromatic substituents. The crossing points of absorbance and emission at 535 nm provide the basis to estimate the singlet excitation energy which is $E_{00} = 2.3$ eV. The reduction potentials of the reference compound **1** and peptide **P1** were measured by cyclic voltammetry (see supporting information). There are two

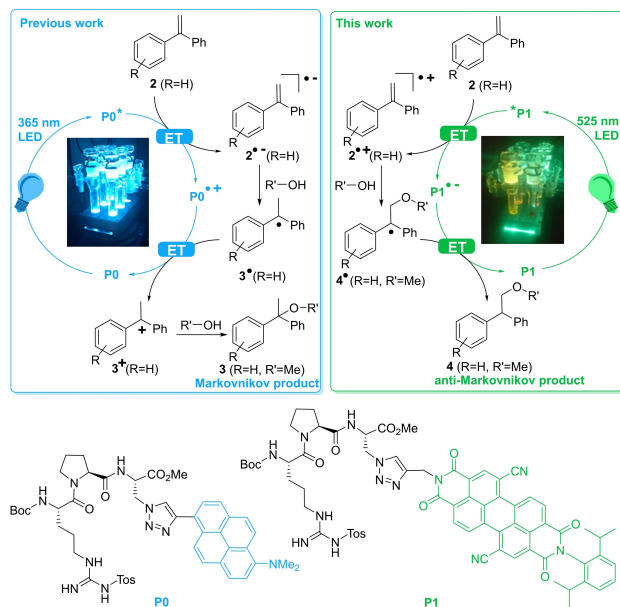


Figure 1. Two different ways of photoredox catalytic activation of alkenes, in particular α -phenyl styrene (**2** with R=H), for nucleophilic addition of alcohols (MeOH, R' = Me): The reduction **2** by the electron-rich *N,N*-dimethylpyrene in peptide **P0** yields the Markovnikov product **3** (left), whereas the oxidation of **2** by the electron-poor 1,7-dicyano-perylene-3,4:9,10-tetracarboxylic acid bisimide in peptide **P1** yields the anti-Markovnikov product **4** (right).

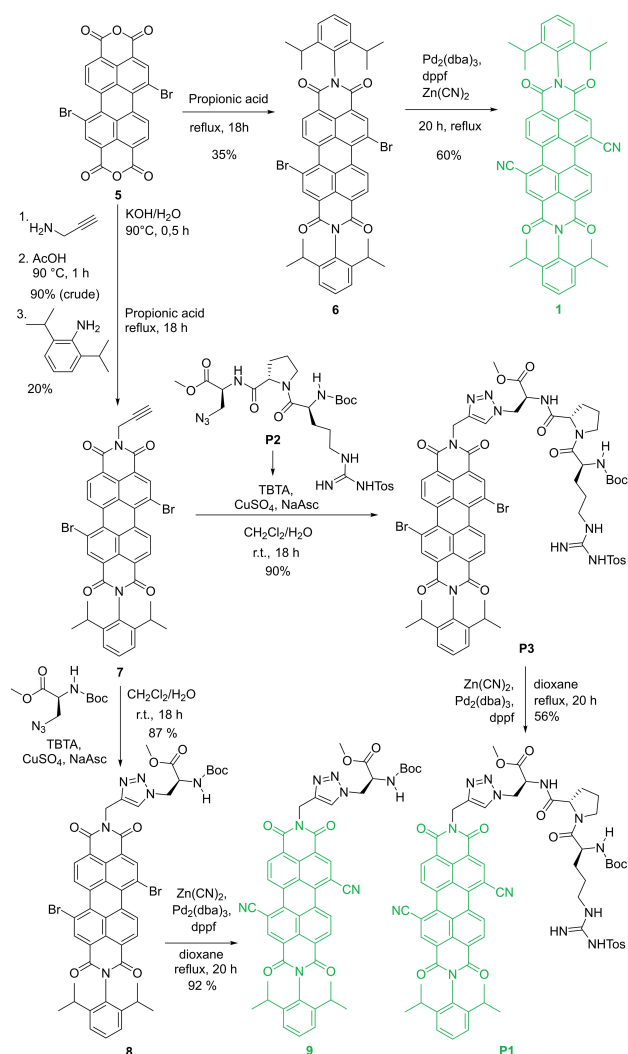


Figure 2. Synthesis of photocatalytically active compounds **1**, **9** and **P1** (Boc-Arg(Tos)-Pro-(CN)₂PBIAla-OMe); TBTA: tris[(1-benzyl-1H-1,2,3-triazol-4-yl)methyl] amin, NaAsc: sodium ascorbate.

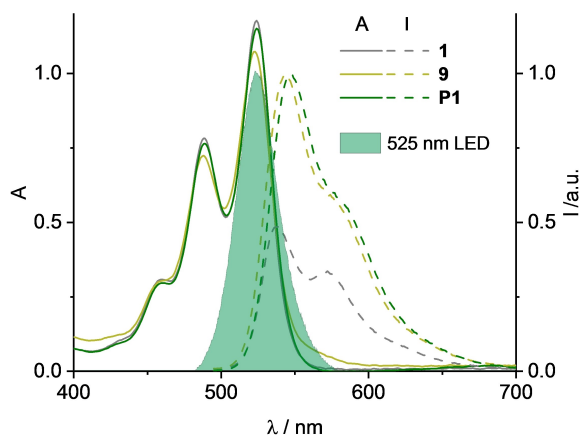


Figure 3. UV/vis absorption and fluorescence of **1**, **9** and **P1** (each 25 μM) in MeCN, r.t., and normalized emission profile of the 525 nm LED.

separate redox potentials for **1** (given vs. SCE), the first for the reduction to the radical anion $1^{\bullet-}$, $E_{\text{red}1}(1/1^{\bullet-}) = -0.15 \text{ V}$, and the second for the reduction to the dianion 1^{2-} , $E_{\text{red}2}(1^{\bullet-}/1^{2-}) = -0.43 \text{ V}$. Compared to $E_{\text{red}1}(\text{P1}/\text{P1}^{\bullet-}) = -0.13 \text{ V}$ and $E_{\text{red}2}(\text{P1}^{\bullet-}/\text{P1}^{2-}) = -0.43 \text{ V}$ for **P1**, it becomes obvious that the peptide environment of the chromophore does not influence the redox behavior. Our reference substrate was α -phenyl styrene (**2**) that has an redox potential for its oxidation of $E_{\text{ox}}(2^{\bullet+}/2) = +1.73 \text{ V}$.^[21] Taken these experimental values together, the driving force ΔG (Gibbs energy) of the photoinduced electron transfer can be estimated by the Gibbs free energy equation, $\Delta G = E_{\text{ox}} - E_{\text{red}} - E_{00} - E_{\text{C}}$ ^[22] Omitting the Coulomb energy, that is presumably very low in polar solvents like MeCN/MeOH, ΔG for the initial photoinduced electron transfer between the photocatalysts **1** or **P1** and the substrate **2** is negative and in the range -0.3 to -0.4 eV .

Fluorescence quenching is a good indication for the initial photoinduced electron transfer between the photocatalyst and the substrate. Accordingly, the fluorescence of **1** and **P1** was measured not only with substrate **2** but also with the derivatives **10–16** that vary by the substituent in para position to the vinyl group (Figure 4). The Stern-Volmer constants K_{SV} were determined and lie in the range between 11.8 M^{-1} and 83 M^{-1} (Table 1). Interestingly, the constants K_{SV} correlate with the Hammett constants σ_{p} that reflect the electronic influence of the substituent R in the substrates **2** and **10–15** ranging from electron-withdrawing (like COOMe in **11**: $\sigma_{\text{p}} = 0.45$) to electron-donating ones (like OMe in **15**: $\sigma_{\text{p}} = -0.27$).^[23] The correlation between σ_{p} and K_{SV} is quite obvious (Figure 5) and support our assumption that the fluorescence quenching of **1** and **P1** by the different substrates is caused by the photoinduced electron transfer as already indicated by the Gibbs free energy calculation and described above. Since **P1** shows stronger fluorescence intensity, the influence by σ_{p} is larger. Taken



Figure 4. Substrates **2**, **10–16** and their methoxylation products **3**, **17–23**.

Substrate (R)	σ_{p} ^[23]	K_{SV} with 1 [M^{-1}]	K_{SV} with P1 [M^{-1}]
2 (H)	0.00	18.9 ± 0.2	28.1 ± 0.5
10 (COOH)	0.45	14 ± 2	10.7 ± 0.7
11 (COOMe)	0.45	15.2 ± 0.6	11.3 ± 0.3
12 (CONH ₂)	0.36	11.8 ± 0.4	25.0 ± 2.0
13 (OCOCH ₃)	0.31	18.0 ± 0.5	27.7 ± 0.5
14 (NHCOCH ₃)	-0.10	26.1 ± 0.1	53.5 ± 0.8
15 (OMe)	-0.27	32.2 ± 0.5	65 ± 3
16 (NMe ₂)	-0.83	64 ± 2	83 ± 4

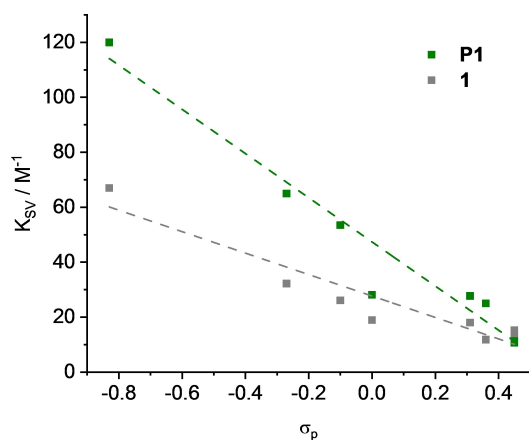


Figure 5. Correlation between the Hammett constants σ_p and the Stern-Volmer K_{SV} constants for substrates **2**, **10–16**. The dashed lines are linear fits ($y = a + b \cdot x$), for **1** and **P1** separately, to illustrate the correlation.

together, these results support the proposed electron transfer between **P1** and the substrates that initiates the photoredox catalytic cycle.

Photocatalytic experiments were performed in a thermostatically controlled reactor block equipped with a 525 nm (green) LED at 25 °C under the exclusion of oxygen. Reaction mixtures were analyzed by GC-MS for product identification and NMR for product quantification with 1,1,2,2-tetrachloroethane as internal standard. Both, **1** and peptide **P1** are highly soluble in MeCN and MeOH due to the 2,6-diisopropylaryl substituents at the nitrogen which allows to run the reaction in MeCN/MeOH mixtures or even pure MeOH. The photocatalytic addition of MeOH to substrate **2** is a very clean reaction using 2.0 mol% of peptide **P1** as catalyst (Table 2). After 15 h

irradiation 29% of substrate **2** are converted to product **3**, after 72 h the reaction is complete and shows 85% yield. Most importantly, the reaction does not need thiophenol or any other additive. The positive influence of the peptide becomes obvious, if the photocatalysis is performed with the reference chromophore **1** or the chromophore-modified amino acid **9**. In both cases, there are only small amounts of product **3** formed (after 15 h irradiation) although significant conversion of substrate **2** was observed. Side products could not be identified. We expect that substrate binding to **P1** (Boc-Arg(Tos)-Pro-(CN)₂PBIAla-Ome) is unspecific. To further elucidate the role of the two amino acids Arg and Pro as part of **P1**, we synthesized the control peptides **P4** (Boc-Gln(Xan)-Pro-(CN)₂PBIAla-Ome) and **P5** (Boc-Arg(Tos)-Gly-(CN)₂PBIAla-Ome). In **P4**, the N-terminal Arg is replaced by a Gln; in **P5** the central Pro is replaced by a Gly. After 15 h irradiation with substrate **2**, both peptides, **P4** and **P5**, give significantly lower yields of product **3** indicating a less efficient substrate binding compared to **P1**. In particular, the missing β -turn induced by Pro in **P5** seems to be critical to the catalytic potency. These results show clearly that peptide **P1** is the best photocatalyst for this reaction, presumably by providing substrate binding.

Further optimization with substrate **2** revealed that the photocatalysis requires only 0.5 mol% **P1** (Table 1), which is a remarkably low photocatalyst loading, and is completed already after 40 h. Using this improved protocol, the substrates **10–12** show quantitative conversions and good yields of 42–100% for the corresponding products **17–20**. These substrates have electron-withdrawing substituents according to their positive Hammett constants σ_p . The other substrates **13–16** show only very low yields, if at all, for the corresponding products **21–23** although some conversion (35–40%) was observed. This was unexpected since these substrates show the most pronounced fluorescence quenching due to their electron-donating substituents. This effect could possibly be explained by the recombination of the initial charge separated state which seems to be faster than the reaction of the substrate radical cations (similar to **2**^{•+}) with MeOH and thus prevents the productive photocatalytic reaction pathway. Instead, other unidentified reactions are taking place to a certain extent, as indicated by the substrate conversion. Nevertheless, these results show clearly, that the concept of photocatalytic peptides works not only for the Markovnikov-type regioselectivity,^[3] but also for this anti-Markovnikov type of nucleophilic addition. The substrate binding, although unspecific, is strong enough to keep the substrate in the vicinity of the perylene bisimide chromophore for forward and, more importantly, backward electron transfer.

We investigated the photocatalysis with substrate **2** by UV/Vis absorption spectroscopy in order to get deeper insights why the photocatalytic reactions with **P1** do not need thiophenol, in contrast to those with **1**.^[16] Remarkably, the UV/Vis absorbance of a reaction solution of **P1** (25 μ M in MeOH) in the presence of substrate **2** (3 mM) shows after a very short time of irradiation (2 min) the nearly complete conversion to the two-electron-reduced radical dianion **P1**²⁻ according to its spectroscopic signature with a characteristic maximum at 605 nm (Figure 6). If

Table 2. Photocatalytic experiments with **P1** (Boc-Arg(Tos)-Pro-(CN)₂PBIAla-Ome), **P4** (Boc-Gln(Xan)-Pro-(CN)₂PBIAla-Ome) and **P5** (Boc-Arg(Tos)-Gly-(CN)₂PBIAla-Ome), ranging from 2 mol% to 0.5 mol%, 40 μ mol substrate in 2 mL MeOH, irradiation by 525 nm LED; yield determined by ¹H-NMR using 1,1,2,2-tetrachloroethane as internal standard, average yield and conversion from four separate experiments.

Photocatalyst	Substrate	Loading [mol %]	Time [h]	Conversion	Product: Yield
1	2	2	15	43%	3 : 5%
9	2	2	15	86%	3 : 18%
P1	2	2	15	38%	3 : 29%
	2	2	40	95%	3 : 80%
	2	2	72	100%	3 : 85%
	2	1	40	100%	3 : 92%
	2	0.5	40	100%	3 : 100%
	10	0.5	40	100%	17 : 67%
	11	0.5	40	100%	18 : 100%
	12	0.5	40	100%	19 : 70%
	13	0.5	40	100%	20 : 42%
	14	0.5	40	40%	21 : - ^[a]
	15	0.5	40	40%	22 : 10%
	16	0.5	40	35%	23 : - ^[a]
P4	2	2	15	75%	3 : 27%
P5	2	2	15	20%	3 : 10%

[a] No product detectable.

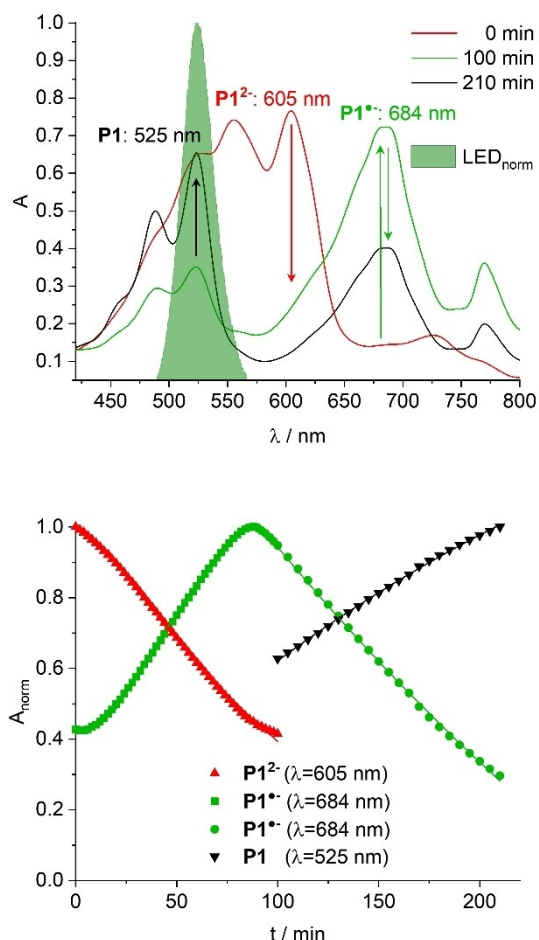


Figure 6. Top: UV/Vis absorption spectra of **P1** (25 μM) with substrate **2** (3 mM) in MeOH after 2 min irradiation by the 525 nm LED ($t=0$ min) and after longer times in the dark ($t=100$ min and 210 min) Bottom: Fitted absorption changes at $\lambda=605$ nm (**P1**²⁻; decay: $\tau=122$ min), $\lambda=684$ nm (**P1**^{*}; growth: $\tau=99$ min; decay: $\tau=270$ min) and $\lambda=525$ nm (**P1**; growth: $\tau=225$ nm); normalized emission profile of the 525 nm LED.

this reaction sample is kept in the dark, the radical dianion **P1**²⁻ decays and concomitantly the radical anion **P1**^{*} rises with a lifetime of 111 min. The characteristic, red-shifted absorbance with a maximum at 684 nm can be assigned to the radical anion **P1**^{*}. The isosbestic point at 630 nm supports that there are no further intermediates until this decay is completed. Afterwards, the radical anion **P1**^{*} decays even more slowly with a lifetime of 248 min and concomitantly, the ground state **P1** is repopulated according to its characteristic fine shape and maximum at 525 nm. Again, an isosbestic point is observed, this time at 550 nm.

We performed similar spectroscopic experiments with a solution of the chromophore **1** (25 μM in MeOH) in the presence of substrate **2** (3 mM). The UV/Vis absorbance of this solution after 2 min irradiation showed the nearly complete conversion to the radical anion **1**^{*}, but not any spectroscopic signature of the dianion **1**²⁻. This is a significant difference to **P1**. Moreover, the radical anion **1**^{*} did not show any significant decay in the dark within 60 min. This indicates that the reaction

partner for the back electron transfer, the radical precursor **3**^{*} of product **3**, was not available for back electron transfer and the formation of the final product **3**. This is the significant difference between the “naked” chromophore **1** and the peptide-chromophore conjugate **P1**. Obviously, the **P1** is able to bind the substrate **2** and the intermediate radical **3**^{*}, until both the fast forward and the slow back electron transfer took place. The “naked” chromophore **1** has not this property and thus an additive, like thiophenol, is needed to promote back electron transfer and to gain efficient photocatalysis.

The formation of the peptide dianion **P1**²⁻ was unexpected and can only be explained by two consecutive electron transfer steps (Figure 7). Both electron transfers to the dianion **P1**²⁻ yield oxidized substrate radical cations **2**⁺⁺ which are trapped by MeOH to the neutral product radicals **3**^{*}. The first electron transfer step forming the charge-separated state **P1**^{*}/**2**⁺⁺ has already been indicated by the fluorescence quenching and the determined Stern-Volmer constant (as described above). For the second electron transfer step, we assume that it requires also separate excitation of the radical anion **P1**^{*} by light; otherwise it is an endergonic reaction according to the redox potentials $E_{\text{red2}}(\text{P1}^{*-}/\text{P1}^{2-})=-0.43$ V and $E_{\text{ox}}(\text{2}^{++}/\text{2})=+1.73$ V. Both, the ground state **P1** and the radical anion **P1**^{*} have significant absorbance in the emission range of the 540 nm LED. The extremely long lifetime of the charge-separated state **P1**^{*}/**2**⁺⁺ provides enough time to allow this second excitation. In the absence of oxygen as reaction partner the decay of **P1**²⁻ as well as the subsequent decay of **P1**^{*} can only be explained by electron transfers to **3**^{*} yielding the final product **3**. The first back electron transfer occurs “less” slow ($\tau=111$ min) than the second electron transfer ($\tau=248$ min). This difference separates the two photoredox catalytic cycles which are coupled by the radical anion **P1**^{*}. The second photoredox catalytic cycle with the radical dianion **P1**²⁻ as intermediate is the mainly operating one for the photocatalytic conversion of substrate **2** to product

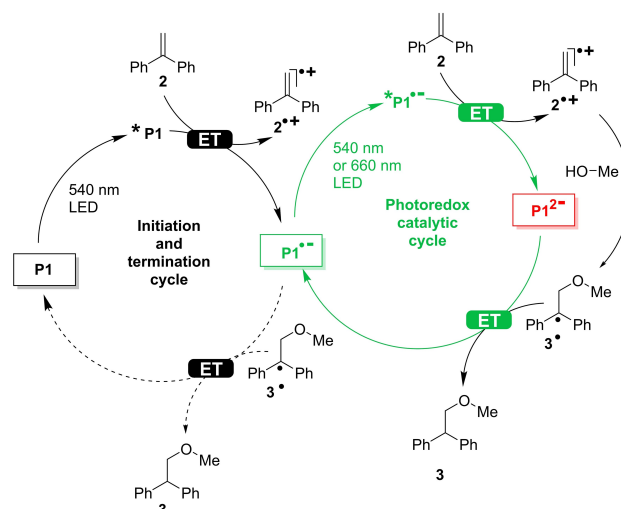


Figure 7. Proposed mechanism of two coupled photoredox catalytic cycles for the nucleophilic addition of MeOH to substrate **2** yielding product **3** in the presence of **P1** as photoredox catalyst. The right and green marked photoredox catalytic cycle is the active one.

3. This is the significant difference of the peptide **P1** and the chromophore **1** as photocatalyst since there is no second photoredox catalytic cycle observable with **1**. The rather slow back electron transfer in this second photoredox catalytic cycle ($\tau = 111$ min) explains why a rather long irradiation time of 40 h is needed for the complete conversion of the substrate **2**. This mechanistic scenario is further supported by an additional experiment. A photocatalytic reaction with substrate **2** and **P1** (0.5 mol%) was first irradiated by the 525 nm LED for only 15 min, which was clearly not sufficient for complete conversion of substrate **2**, but sufficient to form a certain amount of the intermediate radical anion **P1**^{•-}, and subsequently irradiated for 45 min by the 660 nm LED that selectively excites **P1**^{•-}. This alternating irradiation was repeated 40 times (40 h). Complete conversion of substrate **2** could be observed and product **3** was formed in 95 % yield. A similar experiment with a sequence of 15 min irradiation at 525 nm and then 45 min darkness repeated over 40 h, gave only 45 % yield. Taken together, these experiments prove clearly the operating photoredox catalytic cycle with **P1**^{•-} and **P1**²⁻ as photoredox catalyst intermediates.

Conclusion

Forward and backward electron transfer between substrate and photocatalyst are critical parts of photoredox catalytic cycles. The photocatalytic nucleophilic alkoxylation of olefins to products with anti-Markovnikov orientation typically requires an additional reagent (thiophenol) that couples as “electron shuttle” the back electron transfer with product formation and thereby closes the photoredox catalytic cycle.^[16,18] We show by this work that both the fast forward and, more importantly, the slow backward electron transfer steps are controllable by substrate binding to photocatalytically active peptides (“photozymes”). We previously demonstrated this new concept by short proline-rich peptides, such as **P0**, modified with 1-(*N,N*-dimethylamino)pyrene as photoredox catalysts for the nucleophilic addition of alcohols to α -phenyl styrenes into products with Markovnikov orientation. By this work, we complemented the toolbox of “photozymes” by the short peptide **P1** modified with 1,7-dicyano-perylene-3,4:9,10-tetracarboxylic acid bisimide. It photocatalyzes the nucleophilic addition of methanol to α -phenyl styrenes into products with anti-Markovnikov orientation. Our “photozyme” works efficiently without thiophenol by an unconventional mechanism of two coupled photoredox catalytic cycles. The main photoredox catalytic cycle operates via the radical anion and dianion of the **P1** as intermediates. The photoredox catalytic reactions require remarkably low catalyst loadings (0.5 mol%) and yield the methoxylation products in high yields. Although substrate binding is probably unspecific in this case, the concept of “photozymes” for photoredox catalysis has significant potential for other photocatalytic reactions, in particular with respect to enantioselective photocatalysis.

Experimental Section

Materials. All chemicals were purchased from Sigma–Aldrich, Thermofisher, TCI or Carbolution and used without further purification unless otherwise stated. Technical grade solvents, CH₂Cl₂ and *n*-hexane were distilled prior to use. Cyclohexane and EtOAc were purchased on HPLC grade. **5** was prepared via bromination of commercially available 3,4,9,10-perylene tetracarboxylic acid dianhydride.^[24] A mixture of 1,6- and 1,7-regioisomers is formed with the latter being the major product.^[25] As stated in the literature,^[26] these regioisomers exhibit almost the same electronic and optical properties therefore it is neglectable, and only the major 1,7-isomer is shown. β -Azido alanine was prepared following the procedure of Shetty *et al.*^[27] 1-(1-Benzyl-1*H*-1,2,3-triazol-4-yl)-*N,N*-bis[(1-benzyl-1*H*-1,2,3-triazol-4-yl)methyl]-methanamine (TBTA) was synthesized according to literature.^[28] 1,1-Diphenylethylene (**2**) was purchased at *SigmaAldrich*.

Photocatalytic experiments. Experiments were performed under Argon atmosphere. In a usual setup, stock solutions of the substrate (40 μ mol, 1.00 eq.) and catalyst **P1** (0.5 mol%) were added to a Schlenk tube. The solvent was removed under reduced pressure. The vessel was opened under gentle flow of Argon and dry MeOH was added. After closing the vessel, the mixture was cleaned from remaining oxygen by *freeze-pump-thaw* (3 times). Irradiation times varied between 15 h, 40 h and 72 h while the mixtures were stirred. Afterwards, the mixtures were analysed by GC-MS and quantified by NMR using 1,1,2,2-tetrachloroethane as internal standard (singlet at 5.9 ppm, 2H). Every experiment was performed at least in triplicate to report average yields.

General procedure A for the Wittig reaction.^[29] The procedure was performed under argon and exclusion of water. 1.20 eq. of a *n*-BuLi solution (2.5 M in hexane) were added slowly to a stirred suspension of 1.20 eq. methyltriphenylphosphonium bromide in dry THF at 0 °C (ice bath). The mixture was stirred under cooling for 15 min. 1.00 eq. of the corresponding ketone in dry THF was added to the mixture and it was stirred at room temperature overnight (18 h). The reaction was quenched by addition of sat. aqueous NH₄Cl solution. After phase separation, the aqueous phase was extracted three times with EtOAc. The combined organic phase was dried with anhydrous Na₂SO₄. After filtration, the solvent was removed under reduced pressure to obtain the corresponding crude product. Purification by silica gel column chromatography with hexane/dichloromethane as eluent provided the corresponding product.

General procedure B for the synthesis of primary amides. In a dried round-bottom flask 1.00 eq. of the corresponding acid was dissolved in dry THF under Argon atmosphere and cooled to 0 °C in an ice bath. 1.50 eq of thionyl chloride were added slowly under stirring and the mixture was stirred at room temperature for 3 h. The mixture was cooled down to 0 °C again and an excess of aqueous ammonia solution was added carefully. A precipitate (NH₄Cl) was formed. After addition of water, the aqueous phase was extracted with EtOAc (three times), the combined organic phase was dried with anhydrous Na₂SO₄. After filtration, the solvent was removed under reduced pressure to obtain the crude product. It was redissolved in a minimal amount of DCM and crystallized by addition of hexane to obtain the pure product as colourless solid.

General procedure C for Barluenga cross-coupling reaction.^[30] In a dried round-bottom Schlenk flask 1.00 eq. 4-bromobenzoate, 1.00 eq. acetophenone tosyl hydrazone, 0.20 eq. PPh₃, 0.05 eq. Pd₂(dba)₃ and 2.50 eq. K₂CO₃ were suspended in dry dioxane under Argon atmosphere. The mixture was refluxed (ca. 110 °C) for 24 h, a precipitate was formed. After cooling to room temperature, the suspension was diluted with CH₂Cl₂ and filtrated through a celite

pad. The filtrate was freed from the solvent under reduced pressure to obtain the crude product as yellow oil. Purification by silica gel column chromatography (Hex/DCM) yielded the final product as colourless crystals.

General procedure D for saponification of methyl esters.^[3]

1.00 eq. ester derivative was dissolved in THF at 0 °C and 5.00 eq. of LiOH (dissolved in water) was added under stirring. After 5 min the cooling was removed and the mixture was stirred at room temperature. The completion of the reaction was checked by TLC (ethyl acetate). After completion, the mixture was cooled to 0 °C and neutralized with HCl (1 M) and aqueous NaCl solution was added. The aqueous phase was extracted three times with ethyl acetate. The combined organic phase was dried with anhydrous Na₂SO₄. After filtration, the solvent was removed under reduced pressure to obtain the product as colourless solid.

General procedure E for deprotection of Boc-amino derivatives.^[3]

1.00 eq. Boc-protected amine was dissolved in CH₂Cl₂ and 5.00 eq. HCl in dioxane (4 N) were added under stirring. The progress of the reaction is controlled via TLC (CH₂Cl₂). After completion the solvent is removed under reduced pressure to obtain the crude product. The crude product was used directly for the next step without further purification.

General procedure F for peptide coupling.^[3]

In a round-bottom flask 1.00 eq. of the carboxylic acid was dissolved in a mixture of CH₂Cl₂/DMF 6:1 and cooled to 0 °C (ice bath). 1.25 eq. HATU and 2.00 eq. (iPr)₂NEt were added consecutively and the mixture was stirred for 10 min. The amine was pre-dissolved in CH₂Cl₂/DMF and added to the reaction mixture. The mixture was stirred under cooling for 1 h and warmed up slowly to room temperature overnight. After addition of water and dilution with CH₂Cl₂, the organic phase was washed with water (three times), aqueous sat. NH₄Cl (three times), sat. NaHCO₃ (three times) and sat. NaCl (three times) solution. The organic phase was dried with anhydrous Na₂SO₄ and filtrated. The solvent was removed under reduced pressure to obtain the crude product as a yellow to brown oil. Purification by silica gel column chromatography yielded the pure product as colourless solid.

General procedure G for CuAAC. In a round-bottom flask, water was degassed by bubbling with Argon for 15 min. Under stirring 0.30 eq. CuSO₄ and 0.30 eq. TBTA (dissolved in DCM) were added and the mixture was cooled in an ice bath. 0.60 eq. sodium ascorbate were added; a colour change from blue to yellow to colourless due to the formation of the Cu(I)-species was observed. 1.30 eq. of the corresponding azide and 1.00 eq. PBI-alkyne were dissolved in CH₂Cl₂. The solution was added to the in situ generated Cu(I)-species and the mixture was stirred at room temperature overnight. The progress of the reaction was checked via TLC (CH₂Cl₂). After phase separation, the aqueous phase was extracted with CH₂Cl₂ (three times). The combined organic phase was dried with anhydrous Na₂SO₄. After filtration, celite was added and the solvent was removed under reduced pressure to obtain a dry load for silica gel column chromatography. Column chromatography with CH₂Cl₂/acetone or CH₂Cl₂/MeCN yielded the pure product as red solid.

General procedure H for the synthesis of 1. In a dried round-bottom flask 1.00 eq. dibromo-PBI, 10.0 eq. Zn(CN)₂, 0.20 eq. Pd₂(dba)₃ and 0.20 eq. dpfp were suspended in dry dioxane under Argon. The mixture was refluxed (110 °C) for 20 h and diluted with CH₂Cl₂. After filtration through a P4-frit, celite is added to the filtrate and the solvent was removed under reduced pressure. Purification by silica gel column chromatography with CH₂Cl₂/acetone or CH₂Cl₂/MeCN yielded the product as red solid.

Acknowledgements

Financial support by the Deutsche Forschungsgemeinschaft (grant Wa 1386/16-2) and KIT is gratefully acknowledged. We thank the group of Michael Meier (KIT) for providing their GC infrastructure. Open Access funding enabled and organized by Projekt DEAL.

Conflict of Interest

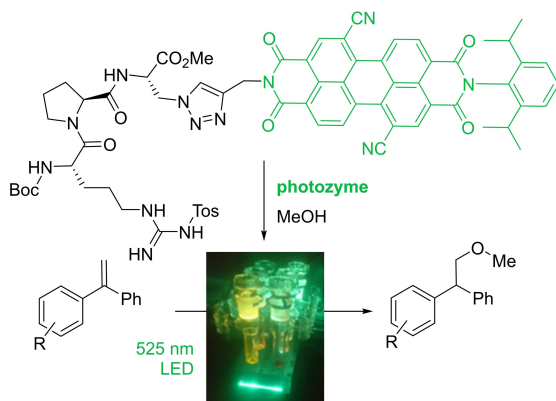
The authors declare no conflict of interest.

Keywords: Alanine · Electron transfer · Fluorescence quenching · Perylene bisimide · Photochemistry

- [1] a) A. J. Metrano, A. J. Chinn, C. R. Shugrue, E. A. Stone, B. Kim, S. J. Miller, *Chem. Rev.* **2020**, *120*, 11479–11615; b) T. Schnitzer, M. Wiesner, P. Krattiger, J. D. Revell, H. Wennemers, *Org. Biomol. Chem.* **2017**, *15*, 5877–5881; c) M. Wiesner, J. D. Revell, S. Tonazzi, H. Wennemers, *J. Am. Chem. Soc.* **2008**, *130*, 5610–5611.
- [2] T. Carell, J. Butenandt, *Angew. Chem. Int. Ed.* **1997**, *36*, 1461–1464; *Angew. Chem.* **1997**, *109*, 1590–1593.
- [3] a) S. Hermann, D. Sack, H.-A. Wagenknecht, *Eur. J. Org. Chem.* **2018**, 2204–2207; b) S. Hermann, H.-A. Wagenknecht, *J. Pept. Sci.* **2017**, *23*, 563–566.
- [4] a) F. Glaser, C. Kerzig, O. S. Wenger, *Angew. Chem. Int. Ed.* **2020**, *59*, 10266–10284; *Angew. Chem.* **2020**, *132*, 10350–10370; b) T. H. Rehm, *ChemPhotoChem* **2019**, *3*, 1–21; c) F. Strieth-Kalthoff, M. J. James, M. Teders, L. Pitzer, F. Glorius, *Chem. Soc. Rev.* **2018**, *47*, 7190–7202; d) D. M. Arias-Rotondo, J. K. McCusker, *Chem. Soc. Rev.* **2016**, *45*, 5803–5820.
- [5] a) S. K. Pagire, T. Föll, O. Reiser, *Acc. Chem. Res.* **2020**, *53*, 782–791; b) N. A. Romero, D. A. Nicewicz, *Chem. Rev.* **2016**, *116*, 10075–10166; c) L. Marzo, S. K. Paigre, O. Reiser, B. König, *Angew. Chem. Int. Ed.* **2018**, *57*, 10034–10072; *Angew. Chem.* **2018**, *130*, 10188–10228; d) G. E. M. Crisenza, D. Mazzarella, P. Melchiorre, *J. Am. Chem. Soc.* **2020**, *142*, 5461–5476; e) L. Capaldo, D. Ravelli, *Eur. J. Org. Chem.* **2020**, 2783–2806; f) D. Ravelli, M. Fagnoni, A. Albini, *Chem. Soc. Rev.* **2013**, *42*, 97–113; g) T. Rigotti, J. Alemán, *Chem. Commun.* **2020**, *56*, 11169–11190.
- [6] a) M. H. Shaw, J. Twilton, D. W. C. MacMillan, *J. Org. Chem.* **2016**, *81*, 6898–6926; b) D. Staveness, I. Bosque, C. R. J. Stephenson, *Acc. Chem. Res.* **2016**, *49*, 2295–2306.
- [7] a) D. P. Hari, B. König, *Chem. Commun.* **2014**, *50*, 6688–6699; b) A. Bosvelli, T. Montagnon, D. Kalaitzakis, G. Vassilikogiannakis, *Org. Biomol. Chem.* **2021**, *19*, 3303–3317.
- [8] B. König, S. Kümmel, E. Svobodová, R. Cibulka, in *Chemical Photocatalysis* (Ed.: B. König), De Gruyter, Berlin, **2020**, pp. 45–71.
- [9] I. Ghosh, L. Marzo, A. Das, R. Shaikh, B. König, *Acc. Chem. Res.* **2016**, *49*, 1566–1577.
- [10] K. A. Margrey, D. A. Nicewicz, *Acc. Chem. Res.* **2016**, *49*, 1997–2006.
- [11] B. Zilate, C. Fischer, C. Sparr, *Chem. Commun.* **2020**, *56*, 1767–1775.
- [12] J. Mateos, F. Rigodanza, A. Vega-Penalosa, A. Sartorel, M. Natali, T. Bortolato, G. Pelosi, X. Companyó, M. Bonchio, L. Dell'Amico, *Angew. Chem. Int. Ed.* **2020**, *59*, 1303–1312.
- [13] C. Rosso, G. Filippini, M. Prato, *Eur. J. Org. Chem.* **2021**, 1193–1200.
- [14] E. Speckmeier, T. G. Fischer, K. Zeitler, *J. Am. Chem. Soc.* **2018**, *140*, 15353–15365.
- [15] a) M. V. Bobo, I. J. J. Kuchta, A. K. Vannucci, *Org. Biomol. Chem.* **2021**, *19*, 4816–4834; b) A. Vega-Penalosa, J. Mateos, X. Companyó, M. Escudero-Casao, L. Dell'Amico, *Angew. Chem. Int. Ed.* **2020**, *60*, 1082–1097.
- [16] M. Weiser, S. Hermann, H.-A. Wagenknecht, *Beilstein J. Org. Chem.* **2015**, *11*, 568–575.
- [17] a) F. Speck, D. Rombach, H.-A. Wagenknecht, *Beilstein J. Org. Chem.* **2019**, *15*, 52–59; b) D. Rombach, H.-A. Wagenknecht, *Angew. Chem. Int. Ed.* **2020**, *59*, 300–303; *Angew. Chem.* **2020**, *132*, 306–310; c) F. Seyfert, H.-A. Wagenknecht, *Synlett* **2021**, *32*, 582–586; d) F. Seyfert, M. Mitha, H.-A. Wagenknecht, *Eur. J. Org. Chem.* **2021**, 773–776.
- [18] N. A. Romero, D. A. Nicewicz, *J. Am. Chem. Soc.* **2014**, *136*, 17024–17035.
- [19] H. Tröster, *Dyes Pigm.* **1983**, *4*, 171–177.

- [20] C. Kohl, T. Weil, J. Qu, K. Müllen, *Chem. Eur. J.* **2004**, *10*, 5297–5310.
- [21] J. Park, Y.-M. Lee, K. Ohkubo, W. Nam, S. Fukuzumi, *Inorg. Chem.* **2015**, *54*, 5806–5812.
- [22] a) D. Rehm, A. Weller, *Ber. Bunsenges. Phys. Chem.* **1969**, *73*, 834–839;
b) D. Rehm, A. Weller, *Isr. J. Chem.* **1970**, *8*, 259–271.
- [23] C. Hansch, A. Leo, R. W. Taft, *Chem. Rev.* **1991**, *91*, 165–195.
- [24] A. Böhm, H. Arms, G. Henning, P. Blaschka, German Patent DE 19547209 A1.
- [25] F. Würthner, V. Stepanenko, Z. Chen, C. R. Saha-Möller, N. Kocher, D. Stalke, *J. Org. Chem.* **2004**, *69*, 7933–7939.
- [26] R. K. Dubey, A. Efimov, H. Lemmetyinen, *Chem. Mater.* **2011**, *23*, 778–788.
- [27] D. Shetty, J. M. Jeong, C. H. Ju, Y. J. Kim, J.-Y. Lee, Y.-S. Lee, D. S. Lee, J.-K. Chung, M. C. Lee, *Bioorg. Med. Chem.* **2010**, *18*, 7338–7347.
- [28] T. R. Chan, R. Hilgraf, K. B. Sharpless, V. V. Fokin, *Org. Lett.* **2004**, *6*, 2853–2855.
- [29] G. Wittig, U. Schöllkopf, *Chem. Ber.* **1954**, *87*, 1318–1330.
- [30] J. Barluenga, P. Moriel, C. Valdés, F. Aznar, *Angew. Chem.* **2007**, *119*, 5683–5686; *Angew. Chem. Int. Ed.* **2007**, *46*, 5587–5590.

Manuscript received: August 31, 2021
Revised manuscript received: October 19, 2021
Accepted manuscript online: October 28, 2021



D. Sack, Prof. Dr. H.-A. Wagenknecht*

1 – 9

**The Concept of Photozymes:
Short Peptides with Photoredox
Catalytic Activity for Nucleophilic
Additions to α -Phenyl Styrenes**



Keep the substrate until "mission is completed": The forward and backward electron transfer steps in a photoredox catalytic cycle are con-

trolled substrate bindings to photocatalytically active peptides, the "photozymes".